Opportunistic Use of In-Vehicle Wireless Networks for Vulnerable Road User Interaction

Pedro M. d'Orey[1], Pedro M. Santos[1], José Pintor[2] and Ana Aguiar[1]

Abstract— In-vehicle wireless networks (e.g., Wi-Fi, Bluetooth) are experiencing a faster market penetration than dedicated V2V technologies and are compatible with non-V2X devices. In this paper, we assess whether commodity in-vehicle networks can leverage opportunistic V2X communication to nodes outside of the vehicle, particularly with Vulnerable Road Users. We characterize the radiation pattern and performance of communication links in the 2.4 GHz band between in-car wireless networks and a wireless-enabled bicycle in two representative interaction scenarios (i.e. parallel and perpendicular vehicle-VRU trajectories) using both production hardware (i.e. built-in WiFi hotspot) and dedicated measurement equipment. Empirical results show that (i) the signal propagation to the outside of the vehicle is strongly affected (up to 20 dB) by the vehicle elements (e.g. pillars) and by the placement of the wireless system inside the car, and (ii) the communication performance (in terms of RSSI, IRT, Throughput) is also impaired by the spatial arrangement of vehicle and VRU, and other time-varying phenomena (e.g., human body and bicycle shadowing). We conclude that the in-car system performance allows supporting a wide range of safety and infotainment applications (e.g., IRT under 300 ms) even at large TX-RX distances, and that the placement of an in-car wireless system should be tailored according to the target application.

I. INTRODUCTION

According to the World Health Organization (WHO) [1], each year millions of people die or are seriously injured as a result of road traffic crashes that have profound socio-economic impacts. In the European Union (EU) [2], nearly half of the road victims are Vulnerable Road Users (VRUs), i.e., pedestrians, cyclists, and motorcyclists. Accidents are mostly caused by driver inattention, lack of situation awareness or misunderstanding the intentions of other road users.

Several solutions based on vehicle sensors (e.g. radar [3] or LIDAR/vision [4]) enable VRU protection through improved environment perception. However, the performance of these systems is often impaired in challenging (urban) scenarios by obstacles (e.g. cars), adverse weather conditions (e.g. snow, fog), among others. Recently, cooperative or cloud-based solutions built over cellular [5], [6] or wireless ad hoc [7], [8] (e.g. 802.11 p or ITS G5 [9]) communication systems

[1] Pedro M. d'Orey, Pedro M. Santos and Ana Aguiar are with Instituto de Telecomunicações, Porto, Portugal and University of Porto, Portugal (e-mail: `pedro.dorey@dcc.fc.up.pt`, {`pmsantos`, `ana.aguiar`}`@fe.up.pt`)
[2] José Pintor is with the University of Porto, Portugal (e-mail: `up201307994@fe.up.pt`)
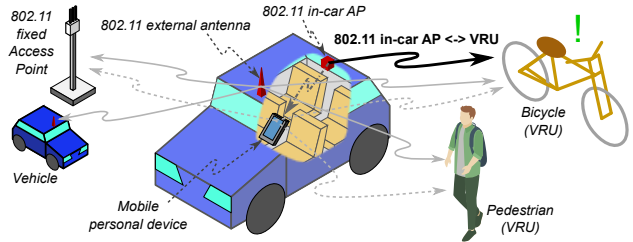
Fig. 1: Communication links between a vehicle node (antenna installed in or out of the vehicle), and other mobile (e.g. VRU or vehicle) or static (e.g. 802.11 fixed Access Point) nodes. The communication link between in-vehicle device and bicycle VRU (depicted in black) presents the distinguishing features.

have been proposed to further improve interaction between drivers and VRUs beyond Line of Sight (LoS) conditions. However, such systems require dedicated equipment (e.g., ITS G5 radio) for both VRUs and vehicles, or cannot meet the stringent requirements (e.g. low latency) of safety applications (e.g. for cloud-based systems).

Nowadays, wireless communications are increasingly used in vehicles to enable in-car (e.g., tire pressure monitoring [10]) or passenger infotainment (e.g. WiFi hotspot) systems. Recent works [11][12] have also shown that in-vehicle communication can enable efficient data offloading, and automotive innovations (e.g. Advanced Driving Assistance, Automated Driving Systems) can explore vehicle-VRU connectivity to substantially mitigate accident rates [13]. We argue that wireless in-car networks, in combination with a communication device installed in the bike (e.g. embedded or smartphone) can enable a wide range of safety [7], efficiency [14] and infotainment applications to improve VRU interaction, while meeting low cost and performance requirements. Improved situational awareness between road users can be achieved by opportunistically monitoring the wireless channel or through dedicated information exchange between nodes[1]. The pervasive availability of smartphones and increasing number of bikes equipped with communication devices allows reducing the system's cost and enables direct communication links between VRUs and vehicles.

We characterize the performance of **vehicle-to-bicycle (V2B) communication links** in the 2.4 GHz band using available in-car wireless devices (i.e. 802.11 b/g) to enable VRU protection and interaction applications. The V2B

---

[1]For instance, the IEEE 802.11 standard mandates that every device transmits periodically beacon frames to allow discovery by other nodes.

communication link presents the following distinguishing features that have not been *jointly* considered in previous V2X studies (see Fig. 1), namely (1) increased shadowing due to additional (moving) objects (e.g. human body, bicycle frame, in-car objects [e.g. headrests, pillars]) leading to fewer Line-of-Sight (LoS) opportunities, (2) additional signal degradation due to antenna location (e.g. inside car as opposed to rooftop V2X antennas) and elevation (e.g. low elevation of VRU device), (3) limitations imposed by the use of production equipment (e.g. as opposed to use of dedicated measurement equipment), (4) mobility of one or both communication nodes (e.g. as opposed to communication to static 802.11 infrastructure [11]) that impairs differently the signal propagation, (5) wide device variability in terms of manufacturers and types (e.g. smartphone or embedded device in bikes), (6) environment (e.g. urban, rural, highway), among others. In this paper, we focus on items (1) to (4) for characterizing and quantifying the performance of the communication system, while items (5) and (6) will be considered in future work.

To achieve this goal, we performed a number of experiments in representative vehicle-VRU interaction scenarios to assess the V2B link quality and some of its distinguishing features using three conventional metrics, namely Received Signal Strength Indicator (RSSI), Throughput and Packet Inter-reception Time (IRT), where the two later metrics inform about the Quality of Service (QoS) offered to VRU protection or interaction applications. To summarize, the main paper contributions are:

- we perform an extensive measurement campaign for characterizing V2B links in two representative scenarios (parallel motion and intersection) and considering different antenna positions;
- through extensive measurements, we study and quantify additional signal attenuation in V2B links caused by the bicycle frame, vehicle structure, and the human body at several TX-RX distances;
- we outline performance metrics for safety and interactive VRU applications.

The remainder of this paper is organized as follows. In Section II, we briefly present the relevant state-of-the-art. Section III describes the experimental evaluation of V2B links. The main results are presented and discussed in Section IV. The concluding remarks are given in Section V.

II. RELATED WORK

In-car communication links. Several previous works analyzed the performance of in-car networks for enabling Wireless Sensor Networks [WSN] (e.g. [15]) and passenger applications (e.g. infotainment using WLAN/Bluetooh [16]). Both works have also analyzed the impact of internal [15] or external [16] interfering devices operating in the 2.4 GHz band, and concluded that the interference level might be considerable. However, few works analyzed the performance of in-car networks operating in the 2.4 GHz band for communication to the exterior of the vehicle. Lin et al. [17] proposed using intra-car WSN for implementing a Blind
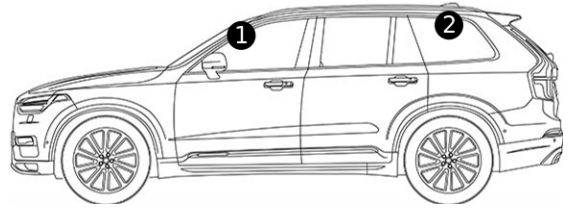

Fig. 2: Side-view of the test car including location of the in-vehicle antennas for the (1) dedicated measurement equipment (DME) and (2) production equipment (PE) setups.

Spot Information System but mostly focused on application development and communication between two cars. More recently, El-Makhour at al.[18] assessed the performance of the Remote Key Entry and Hands Free systems that operate in the 125 kHz and 434 MHz bands.

V2X link characterization. Channel characterization and link performance in V2X communication has been reported for a variety of technologies and typically associated frequencies (e.g., 802.11b/g [19] and 801.15.4 [20] in the 2.4 GHz band, 802.11 p in the 5.9 GHz band [21]), and scenarios (e.g., highway [22], intersection [23]). Gass et al. [19] and Wellens et al. [22] describe the performance of UDP and TCP wireless transfers over 802.11b links between a mobile device in a moving car and an infrastructural access point. Karedal et al. [21] characterize the wireless channel in urban intersections regarding power delay profile (PDP), channel gain and delay spread for the 5.6 GHz center frequency. The authors of [23] evaluate the performance of 802.11 p systems in two corner interaction scenarios - blind (building) and semi-blind (forested) - in terms of packet loss ratio. Lin et al. [20] characterize the communication in terms of RSSI and PDR between a scooter and another vehicle using IEEE 802.15.4 short-range communication radios.

Antenna placement for V2X communications. Several works have demonstrated the impact of the antenna placement on the performance of the communication system. The work of [24] reports (via simulation) the radiation patterns of antennas mounted on the exterior of a vehicle. The 3D radiation pattern of an antenna installed on the left rear-view mirror (obtained via simulation) is presented in [25]. Empirical radiation patterns for several positions in the rooftop of a private vehicle are described in [26]. Kukolev et al. [27] perform a similar study in an indoor scenario for a TX antenna mounted on the rear of the rooftop.

Our approach differs from previous work as it leverages production **in-car communication systems** for passenger use – the in-car WiFi device – **for communication with exterior wireless terminals** (Fig. 1). Such systems were not designed for that purpose, but implement technologies commonly available in the personal devices of pedestrians, cyclists or other VRUs. To the best of our knowledge, no other previous work has extensively characterized the communication performance of in-car 802.11 b/g networks operating in the 2.4 GHz band with links to external terminals, namely bicycles.

III. Experimental evaluation of V2B links

A. Experimental platform

The measurement system was installed in a vehicle (Volvo XC90) and a conventional bicycle. We consider two setups for the in-car WiFi network: 1) production WiFi equipment (PE) already available in the vehicle and 2) dedicated measurement equipment (DME). A DME was also installed on the bicycle. A laptop and a GPS receiver (Globalsat BU-353S4) were installed in both nodes for capturing packets and collecting statistics, timing and position information (1 Hz frequency).

The measurement system uses 802.11 b/g standard complaint radios operating in the 2.4 GHz frequency band, namely devices produced by ACTIA for the PE setup and TP-Link TL-WN722N devices for the DME setup. The default transmit power is 18 dBm for PE and 20 dBm for DME. The locations of the in-vehicle antennas are depicted in Fig. 2. For the PE setup, according to available documentation, a Connectivity Control Unit (CCU) with an integrated 802.11 antenna is installed in the vehicle roof under the external shark fin antenna. The in-vehicle antennas are installed at a height of around 1.6 m. For the DME setup, omni-directional 4 dBi gain antennas are installed vertically under the box supporting the rear-view mirror. The same antenna is installed in the middle of the bicycle handlebar at a height of approximately 0.95 m; this position has been identified in a previous study [28] as one of the most promising to support a variety of Bicycle-to-Bicycle (B2B) applications due to its almost isotropic radiation (when cyclist is absent) as shown in Fig. 6 and because bike smartphone mounts are typically installed in this location.

To assess the performance of the V2B communication link, we conducted several experiments resorting to:

1) **Periodic Beaconing:** Many VRU safety protection systems resort to beacons broadcasted by the communication system. The PE and DME systems transmit beacons about every 100 ms at the lowest available mandatory data rate (i.e. 1 Mbps whenever mode b is enabled). The size of the beacon packet is 214 Bytes. Beacons are stored at the transmitter and at the receiver for gathering RSSI measurements to assess the link quality, and how it is impaired by the human body and the vehicle structure.

2) **Continuous Data Transfer:** To assess infotainment and efficiency applications (e.g. audio streaming), we also perform throughput measurements using the *iperf* (https://iperf.fr/) active network measurement tool. UDP datagrams were transmitted from the bicycle (source) to the vehicle (sink)[2] with a high but variable transmission period. The datagrams size was 1470 bytes and the offered load was 56 Mbps. Source and sink nodes store transmitted and received packets using *tcpdump* for gathering RRSI measurements, and also the logs generated by the *iperf* measurement tool.

[2]We assume that there exists a strong degree of symmetry to the reciprocal B2V link as show in previous studies assessing V2X links [29].

Fig. 3: Experiments were performed in a surface parking lot. The bicycle route depicted in yellow was followed several times (length: 400 m).

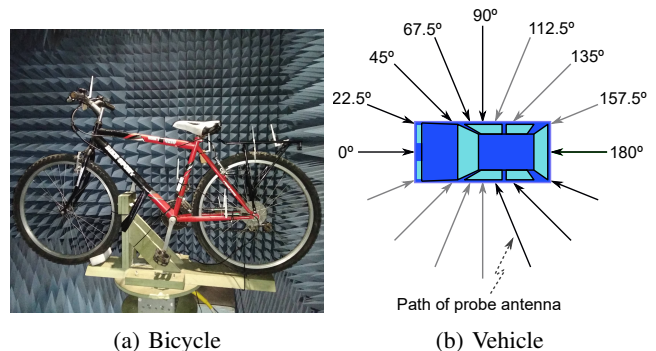(a) Bicycle   (b) Vehicle

Fig. 4: Rough Estimation of Bicycle and Vehicle Radiation Pattern, respectively: (a) measured in anechoic chamber with static TX and RX antennas; (b) measured in the test site where arrows indicate the trajectory of the mobile RX probe antennas (mounted on two bikes) moving towards static TX vehicle.

The data rate is automatically adapted by the device in the range [1-54] Mbps for 20/22 MHz channels using a manufacturer's proprietary algorithm.

B. Experiments Test Site

The measurement campaign was conducted during July 2018 in Porto, Portugal. Experiments were performed in a surface parking lot (Fig. 3) with length of approximately 400 m, where there predominantly exists Line of Sight (LoS) conditions between the transmitter and receiver, and the number of surrounding objects (e.g. vehicles, foliage or buildings) is low reducing reflection, diffraction and scattering of electromagnetic waves. During the measurements, the vehicle was kept static at the center of the parking lot (41.21668, -8.71309) and the bicycle followed several times the route shown in Fig. 3.

C. Estimating Bicycle and Vehicle Radiation Patterns

Previous work has shown that obstacles (e.g. vehicles [30], human body) cause severe fading to V2X links. However, such measurements do not characterize accurately fading conditions experienced by V2B links due to the aforementioned specificities of this communication link. Thus, we performed a set of experiments to evaluate fading induced by

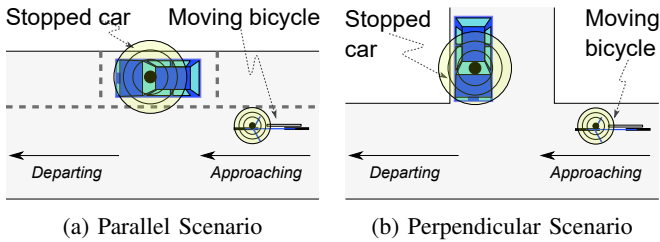(a) Parallel Scenario   (b) Perpendicular Scenario

Fig. 5: Measurement scenarios

the (1) bicycle frame and (2) vehicle elements, measuring the received signal strength at different angles around the object. At each angle, the experimental platform collects at least 40 RSSI samples resorting to *Periodic Beaconing* (i.e. the vehicle communication unit periodically transmitted beacon frames that were captured by the bicycle communication unit), which are averaged to estimate the directivity patterns.

Bicycle Radiation Pattern (Fig. 4a): The experiments were carried out in an anechoic chamber where the distance between TX and RX nodes was roughly 4.5 m. The TX DME node was installed in a non-conducting stand, while the bicycle frame with an RX DME device installed in the center of the handlebar was attached to a rotating stand that moved clockwise 360° in 5° increments. For comparison purposes, similar experiments were conducted to estimate the directivity pattern of the DME bare antenna.

Vehicle Radiation Pattern (Fig. 4b): The experiments were executed in the test site described in Section III-B. The TX PE and DME nodes were installed inside the test vehicle in the positions shown in Fig. 2, while RX DME nodes were attached to two bicycles. The test vehicle was placed at the center of the test site (with a given angle with respect to a bike's path) and two bicycles were driven following the route depicted in Fig. 3. The procedure was repeated several times after rotating the vehicle into different angles (e.g. 22.5°).

D. Measurement Scenarios

To assess the feasibility of using in-vehicle networks for VRU protection and interaction, we consider two critical interaction scenarios between vehicles and bikes that have been identified in studies analyzing historical accident data [31]:

- **Parallel** (Fig. 5a): the vehicle and the VRU travel in the same or opposite directions. Common situations include a car door opening or a vehicle invading the bike's path.
- **Perpendicular** (Fig. 5b): the vehicle and the VRU travel in different road segments towards or away from a conflict area. This scenario replicates an intersection or junction where the likelihood of an accident is higher.

We conducted an extensive measurement campaign in the designated test site to assess each of the presented scenarios resorting to both *Periodic Beaconing* and *Continuous Data Transfer*. For statistical significance reasons, we performed at least 3 measurements rounds for each parameter set: 1) scenario type (i.e. parallel or perpendicular), 2) setup (i.e. DME or PE), and 3) direction (e.g. approaching or departing). Each aggregated measure (e.g. average RSSI for
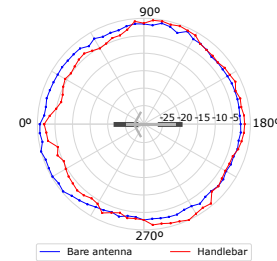

Fig. 6: (Bicycle) Azimuthal Directivity Patterns of the DME setup measured in an anechoic chamber for: 1) bare (quasi omnidirectional) antenna and 2) antenna placed on the center of bicycle handlebar. Measurement values were re-scaled with reference to the maximum RX power.

a given distance bin in Fig. 9) was computed using at least 40 samples.

E. Metrics

We resort to the following three metrics to characterize communication between vehicles and bicycles:

- **Received Signal Strength Indicator (RSSI)**: characterizes the power level of the radio signal at the receiving end after propagation through the wireless channel, which is impaired by moving or static obstacles, system configurations (e.g., antenna location and height), among other factors. This metric describes the link quality between transmitter and receiver nodes.
- **Throughput**: the maximum rate at which the wireless channel capacity is used for data transmission, i.e. the successful message delivery rate over the wireless channel. This metric is specially relevant for infotainment (e.g. multimedia) or efficiency (e.g. map updates) applications.
- **Beacon Inter-Reception Time (IRT)**: the time interval between consecutive successfully received beacon packets. This metric is important for safety critical applications enabled by periodic beaconing.

IV. RESULTS

A. Angular dependency of RSSI: impact of structure

Bicycle Radiation Pattern: Fig. 6 shows that, as expected, the radiation pattern of the bare antenna is quasi omnidirectional in the horizontal plane. The results also demonstrate the impact of the bicycle frame on the radiation pattern of the DME setup when comparing with the bare antenna radiation pattern, impairing the signal propagation in a wide subset of angles (e.g. range between 0°-90°) and slightly enhancing the signal in a smaller range of angles (e.g. range between 225°-270°). Thus, the antenna gain mostly reduces up to 5 dB in the horizontal plane due to effect of the bicycle frame that reflects electromagnetic waves.

Vehicle Radiation Pattern: Figs. 7a and 7c depict the radiation pattern of the in-vehicle 802.11 antennas for the DME and PE setups, respectively, for communication to a node outside of the vehicle. Each data point represents the normalized average RSSI for a given angle and TX-RX

(a) DME setup - Norm. avg.   (b) DME setup - Std. dev.

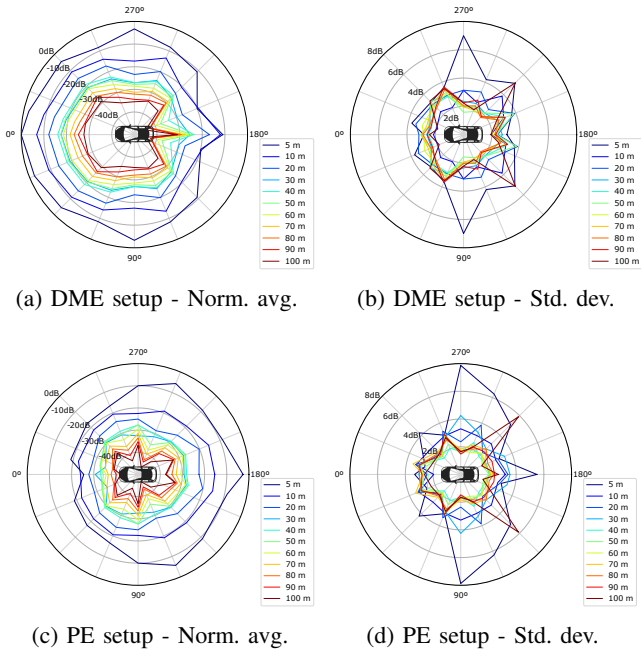(c) PE setup - Norm. avg.   (d) PE setup - Std. dev.

Fig. 7: Normalized average RSSI (left) and standard deviation (right) of measured RSSI for the DME and PE setups installed in the car, and different TX-RX separations. The vehicle's front is aligned with the angle 0°. Additional resolution provided in the [0,10m] range due to larger differences in the spatial configuration of car elements and antenna at close distances.

separation. The normalization is performed by subtracting the maximum average RSSI value (i.e. -35.76 dBm for the DME setup for 0° angle and 5 m bin) from all remaining measurements. Note that we normalize all values with respect to the first distance bin. The standard deviation of the measured RSSI values shown in Figs. 7b/7d exhibits large deviation at short distances specially at the 90° and 270° for both setups; in the PE setup also large deviations occur for communications towards the back of the vehicle. In general, the RSSI standard deviation metric decreased progressively for larger TX-RX distances.

The presented results show that - for both setups - the transmitted signal does not equally propagate to the exterior of the vehicle despite the quasi omni-directional pattern of the DME setup (as shown in Fig. 6). We argue that this phenomena mainly occurs due the vehicle's elements (e.g. pillars) that impair signal propagation to outside of the vehicle leading to pronounced shadowing for selected angles. For a given distance, the average signal attenuation can vary for the considered angles between 12.1-20.9 dB for the DME setup and 6.4-17 dB for the PE setup. In addition, the existence of metallic (e.g. car roof) and non-metallic elements (e.g. sunroof in the test vehicle) can influence the antenna's directivity pattern as previously reported in [32] and [33]. The results also suggest that, for a given angle and setup, the level of obstruction varies for different TX-RX distances due

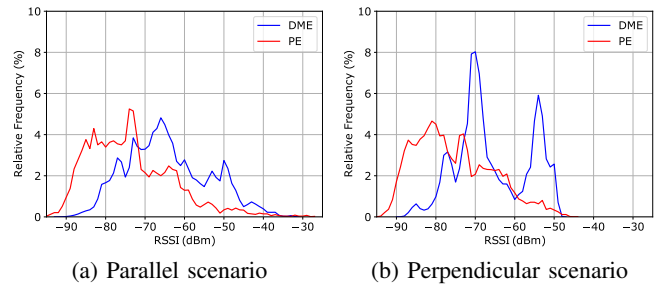(a) Parallel scenario   (b) Perpendicular scenario

Fig. 8: Empirical Distribution Function of Received Signal Strength Indicator (RSSI) for two scenarios using PE and DME setups.

to increased shadowing caused by additional obstructions, for instance, due to the lower height of the bicycle antenna. For instance, for the PE setup, the pattern is fairly omni-directional at low TX-RX separation, while a more star-like pattern is evidenced for higher node separations.

Comparing both setups, we observe that the DME setup favors propagation to the vehicle's front, while the PE setup favors propagation to the vehicle's back and, at higher TX-RX distances, also to perpendicular directions (i.e. 90° and 270°). These results can be attributed to the antennas' location (front and rear of vehicle for DME and PE setups, respectively) and varying level of obstruction of the path between transmitter and receiver. The distance between the isolines sharply decreases with increasing TX-RX separation due to the pronounced decrease of the signal strength.

B. Parallel and Perpendicular Interaction Scenarios

Received Signal Strength Indicator (RSSI): Fig. 8 depicts the RSSI empirical distribution function for the parallel and perpendicular scenarios for the PE and DME setups. For the parallel scenario (Fig. 8a), the results show that the RSSI distributions for both setups are similar but offset by approximately 12 dB. We attribute this to the lower transmission power, larger cable losses and the less favorable antenna position of the PE system for communication to outside of the vehicle as show in Section IV-A, which leads to fewer Line of Sight (LoS) conditions due to obstacle obstruction and bicycle mobility. Similar results are obtained for the perpendicular scenario despite the more pronounced peaks at approximately -55 and -70 dBm.

Fig. 9 shows the RSSI as a function of distance for vehicle-to-bike communication. As expected, the RSSI decreases sharply according to the power law function as the distance between communicating nodes increases. Analyzing a given scenario and setup (e.g. Fig 9a), we distinguish the situation when the Bike and Cyclist set (BCS) is approaching or departing from a defined vehicle position (e.g. car's front); note that in the *departing* direction the BCS will often block the path between the communication nodes due to the location of the bicycle's antenna (installed at center of bicycle handlebar). We observe that shadowing induced by the human body and the bicycle frame causes the received signal power to decrease by approximately 10-19 dB due to

(a) Parallel with DME   (b) Perpendicular with DME
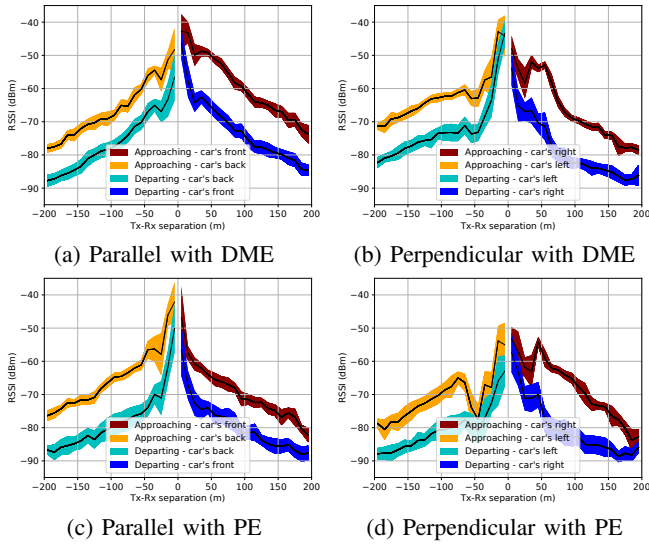

(c) Parallel with PE   (d) Perpendicular with PE

Fig. 9: Received Signal Strength Indicator (RSSI). For each 10 m distance bin, we represent the mean RSSI and the corresponding one standard deviation around the mean.

(a) Parallel scenario   (b) Perpendicular scenario

Fig. 10: Throughput as a function of distance for DME. Each point corresponds to the average throughput per 1 s interval.

(a) Parallel scenario   (b) Perpendicular scenario

Fig. 11: Histogram of negotiated nominal rates per distance bin (10 m wide) for the DME setup. The radius of the circles is proportional to the frequency for each of the 4 considered interaction use cases.

the loss of LoS conditions for a wide range of angles between transmitter and receiver nodes, other signal impairments (e.g. scattering), etc.; these results are larger than the ones reported in [20] that considered static conditions. The absence of the symmetry between both sides of the curves might be attributed to irregularities in the radiation pattern or asymmetries in the vehicle's structure, as also reported in [34]; for the DME setup this effect also occurs due to the slightly shifted antenna installation with regard to the vehicle's transversal center. We also observe significant quick signal fluctuations over short distances even for LOS channels. These quick fluctuations might be attributed to *Two-Ray Interference* [35] of a ground reflection causing constructive and destructive signal interference at the receiver.

The relative performance of the two setups becomes apparent by observing good RSSI performance (larger values throughout range) at the front-mounted DME setup when the bicycle approaches the car front (Fig. 9a, red dataset) and, reciprocally large RSSI values at the rear-mounted PE setup when the bicycle approaches the car's rear (Fig. 9c, yellow dataset). In the perpendicular scenario, the RSSI metric is lower for the PE setup when comparing with the DME setup due to the different configurations detailed previously. This is especially evident for the approaches/departures from the front (parallel scenario) / right (perpendicular scenario) of the vehicle that might be attributed to the antenna installation at the rear of the vehicle.

Throughput: Fig. 10 depicts the Throughput metric as a function of distance for the DME setup[3]. The results show that, both parallel and perpendicular scenarios, nodes can successfully exchange large amounts of data up to at least around 150 m for experiments without human body

[3]Results are not available for the PE setup because it was not possible to inject traffic without interfering with the experiments.
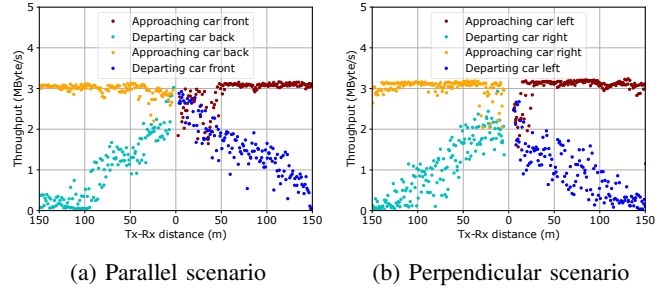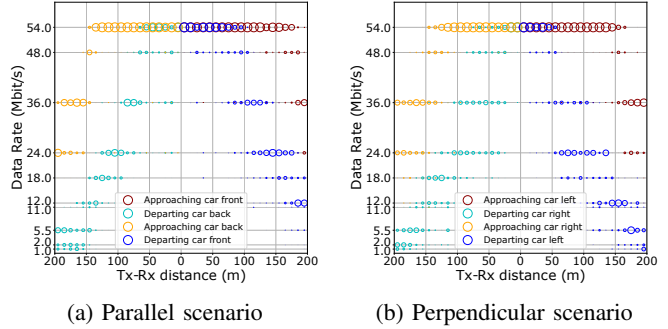
and vehicle induced shadowing (i.e. Figs. 10a and 10b, yellow and brown datasets). On the other hand, experiments with reduced effective received signal power (e.g. due to human body shadowing) suffer from a sharp decrease of throughput as the node distance increases (i.e. Figs. 10a and 10b, blue and green datasets) due to the more aggressive rate adaptation as shown in Fig. 11. The more challenging propagation conditions reduce the maximum communication range for infotainment applications to below 100-150 m, and an even smaller effective range depending on the application requirements (e.g. apps requiring a given minimum throughput for sustainable operation). Comparing both scenarios, we also observe that the throughput results are quite similar.

Fig. 11 presents the frequency of negotiated nominal data rates per any given TX-RX distance for both scenarios. In the parallel scenario, during the approaching stages (front or rear), the terminals agree on the highest data rate even at a distance of 150 m; in the departing stages, negotiated data rates start a linear decreasing trend from the highest value as soon as TX-RX distance reaches 50 m and until the maximum range measured (200 m). The parallel and perpendicular scenarios exhibit similar trends having the perpendicular case slightly lower values than those of the parallel case. This is consistent with the behaviour of the actual throughput samples of Fig. 10; it also indicates that negotiated data rate or throughput may not be a good indicators of terminal proximity in ranges of interest for
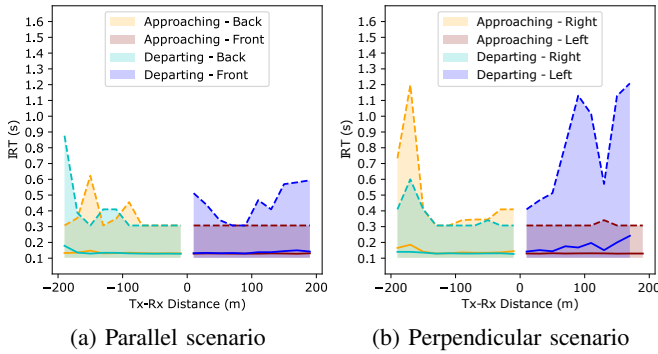
| | (a) Parallel scenario | (b) Perpendicular scenario |

Fig. 12: Mean (——) and 99th percentile (– –) of the Beacon Inter-reception Time (IRT) for the Parallel and Perpendicular scenarios measured using Production Equipment (PE).

critical scenarios (i.e., below 100 m).

Beacon Inter-Reception Time (IRT): Fig. 12 depicts the mean and 99th percentile of the Beacon Inter-Reception Time (IRT) measured using the PE setup for the parallel and the perpendicular scenarios. Recall that beacons are sent about every 100 ms and that larger IRT values are due to lost packets. The results show that the average and the 95th percentile of the IRT are around 100 ms and 300 ms in for all scenarios except the *Departing - Left* case for the Perpendicular scenario. As expected, the IRT increases with the TX-RX separation due to the more challenging propagation conditions; this result is specially evident for the *Departing* cases in both scenarios. Analyzing, the worst case scenario (99th percentile), we note that values of the IRT increase considerably (up to 1.2 s) but this mostly occurs at larger TX-RX distances, which are less relevant for VRU protection systems. Given the results presented in the previous sections, we argue that the performance of the DME would even be more favorable in terms of IRT.

The results show that on average the probability of burst errors is low, which suggests that the system is able to support safety applications with stringent time requirements at short node separations given the low probability of awareness blackouts (i.e. high IRT values), especially in the parallel scenario and for LoS conditions (i.e. approaching situations without shadowing induced by the human body and bicycle frame). Increasing the beacon frequency would certainly further decrease the IRT metric in most situations. According to [36] the average and 99th percentile of travel speed on roadways for electric bike users are 13.3 km/h and 32 km/h, respectively, which translates - on average and worst case scenarios - into 1 m and 10.7 m without updated situational awareness information at large TX-RX distances, respectively. Note also that the likelihood of burst errors is even lower when nodes are in close proximity, which is critical for safety applications.

C. Discussion

Our empirical results show that an in-vehicle communication system can be opportunistically used to support a variety of safety (e.g., collision warning), efficiency (e.g.

data offloading) and infotainment applications for VRU interaction, specially in the most relevant scenario where the bicycle approaches a car (parallely or perpendicularly): the PE setup can offer a IRT below 300 ms (95th percentile), and the throughput attained by the DME (an in-car setup favouring forward communication) is around 3 MBytes/s. We also observed that human and vehicle structure shadowing, and the scenario type affect the link quality and the system performance in terms of throughput and IRT, which indicates that different communication configurations may be necessary depending on the vehicle-VRU spatial arrangement.

In the parallel scenario, we observe better RSSI performance from a front- or rear-mounted setup when the bicycle approaches the car front or rear, respectively; in the perpendicular scenario, the PE setup exhibits a performance degradation of the RSSI and IRT metrics (w.r.t. the parallel scenario) that is consistent with the more reticulated radiation patterns measured for the PE setup and its rear-mounted position. Both observations stress the profound impact of the vehicle's structural elements (i.e., pillars) and interior objects (e.g., headrests) in the performance of in-car wireless networks. Our work clearly highlights that placement of in-car wireless systems should be tailored to the target applications, e.g., collision avoidance at intersections should favour forward-facing setups.

Contrary to ITS-G5 networks, there does not exist a *common* channel in WiFi (e.g. Control Channel in ITS-G5) where nodes can exchange (time-critical) information. On the other hand, the interference created by other devices operating in the 2.4 GHz should be taken into consideration. Thus, a timely and practical solution to achieve convergence on a 802.11 b/g channel common to car and VRU remains open for discussion. The wide variety of channels that production on-board WiFi systems may utilize requires, for instance, the cyclist's device to perform active scanning over all channels. OEMs could agree on a standardized channel and beacon rate that VRUs may monitor, or on zone-based solutions where (crowdsourced) channel interference data is gathered to assist on the (collective) selection of the best channel to exchange information. However, such solutions might be costly and/or impractical, and further research is required.

V. CONCLUSIONS

We evaluated the performance of 2.4 GHz links between in-car wireless networks and bicycles equipped with commodity wireless devices in two representative interaction scenarios. We characterize how the vehicle's structural elements and interior objects contribute to non isotropic radiation pattern, as opposed to the rooftop-mounted external antennas. We conclude that in-car networks can support selected safety and infotainment applications for VRU interaction given the system's performance in terms of high throughput and low latency, while keeping the system's costs low. The results also show that the performance of an in-car wireless system can differ w.r.t to its placement within the car, and system placement should be driven by the target applications.

As future work, we aim at assessing the system performance for different system configurations, vehicle types, and scenarios (e.g. in urban areas with predominant non-LoS conditions and additional shadowing due to vehicles and buildings). We also intend to also quantify the signal attenuation caused by in-vehicle passengers, and evaluate scenarios with varying levels of background traffic (e.g. generated by in-car passengers or other road users).

REFERENCES

[1] W. H. Organization, *Global status report on road safety 2015*. World Health Organization, 2015.

[2] European Commission, "Road safety in the European Union: Trends, statistics and main challenges," Brussels, Belgium, March 2015.

[3] E. Schubert, F. Meinl, M. Kunert, and W. Menzel, "High resolution automotive radar measurements of vulnerable road users – pedestrians amp; cyclists," in *IEEE Conference on Microwaves for Intelligent Mobility*, April 2015, pp. 1–4.

[4] C. Premebida, G. Monteiro, U. Nunes, and P. Peixoto, "A Lidar and Vision-based Approach for Pedestrian and Vehicle Detection and Tracking," in *IEEE Intelligent Transportation Systems Conference*, Sept 2007, pp. 1044–1049.

[5] I. de-la Iglesia, U. Hernandez-Jayo, and J. Perez, "CS4VRU: A Centralized Cooperative Safety System for Vulnerable Road Users Using Heterogeneous Networks," in *IEEE Vehicular Technology Conference*, Sept 2015, pp. 1–5.

[6] W.-L. Jin, C. Kwan, Z. Sun, H. Yang, and Q. Gan, "SPIVC: A Smartphone-based inter-vehicle communication system," in *Transportation Research Board Annual Meeting*, 2012.

[7] J. Anaya, E. Talavera, D. Giménez, N. Gómez, J. Felipe, and J. E. Naranjo, "Vulnerable Road Users Detection Using V2X Communications," in *IEEE Intelligent Transportation Systems Conference*, Sept 2015, pp. 107–112.

[8] J. Santa, P. J. Fernández, and M. A. Zamora, "Cooperative ITS for Two-wheel Vehicles to Improve Safety on Roads," in *IEEE Vehicular Networking Conference*, Dec 2016, pp. 1–4.

[9] M. Boban and P. M. d'Orey, "Exploring the Practical Limits of Cooperative Awareness in Vehicular Communications," *IEEE Transactions on Vehicular Technology*, vol. 65, no. 6, pp. 3904–3916, June 2016.

[10] R. M. Ishtiaq Roufa, H. Mustafaa, S. O. Travis Taylora, W. Xua, M. Gruteserb, and et al., "Security and Privacy Vulnerabilities of In-car Wireless Networks: A Tire Pressure Monitoring System Case Study," in *USENIX Security Symposium*, 2010, pp. 11–13.

[11] V. Bychkovsky, B. Hull, A. Miu, H. Balakrishnan, and S. Madden, "A Measurement Study of Vehicular Internet Access Using in Situ Wi-Fi Networks," in *Int. Conference on Mobile Computing and Networking*, Los Angeles, CA, USA, 2006, pp. 50–61.

[12] N. Cheng, N. Lu, N. Zhang, X. S. Shen, and J. W. Mark, "Vehicular WiFi Offloading: Challenges and Solutions," *Vehicular Communications*, vol. 1, no. 1, pp. 13 – 21, 2014.

[13] M. Blanco, J. Atwood, S. Russel, T. Trimble, J. McClafferty, and M. Perez, "Automated vehicle crash rate comparison using naturalistic data," Virginia Tech Transportation Institute, Tech. Rep., 2016.

[14] S. Céspedes, J. Salamanca, A. Yañez, C. Rivera, and J. C. Sacanamboy, "Platoon-based Cyclists Cooperative System," in *IEEE Vehicular Networking Conference*, Dec 2015, pp. 112–118.

[15] J. Lin, T. Talty, and O. K. Tonguz, "An Empirical Performance Study of Intra-vehicular Wireless Sensor Networks under WiFi and Bluetooth Interference," in *IEEE Global Communications Conference (GLOBECOM)*, Dec 2013, pp. 581–586.

[16] A. Mourad, S. Muhammad, M. O. A. Kalaa, H. H. Refai, and P. A. Hoeher, "On the performance of WLAN and Bluetooth for in-car infotainment systems," *Vehicular Communications*, vol. 10, pp. 1 – 12, 2017.

[17] J. Lin, T. Talty, and O. K. Tonguz, "Feasibility of Safety Applications Based on Intra-Car Wireless Sensor Networks: A Case Study," in *IEEE Vehicular Technology Conference*, San Francisco, USA, Sept 2011, pp. 1–5.

[18] R. El-Makhour, M. Gatsinzi-Ibambe, X. Bunlon, and P. Boutier, "Overview of Radiofrequency Simulation for Automotive Antennas at Renault," in *European Conference on Antennas and Propagation (EuCAP)*, Lisbon, Portugal, April 2015, pp. 1–5.

[19] R. Gass, J. Scott, and C. Diot, "Measurements of In-motion 802.11 Networking," in *IEEE Workshop on Mobile Computing Systems and Applications*. IEEE, 2005, pp. 69–74.

[20] H.-M. Lin, H.-M. Tsai, and M. Boban, "Scooter-to-X communications: Antenna placement, Human Body Shadowing, and Channel Modeling," *Ad Hoc Networks*, vol. 37, pp. 87 – 100, 2016.

[21] J. Karedal, F. Tufvesson, T. Abbas, O. Klemp, A. Paier, L. Bernadó, and A. F. Molisch, "Radio channel Measurements at Street Intersections for Vehicle-to-vehicle Safety Applications," *IEEE Vehicular Technology Conference*, 2010.

[22] M. Wellens, B. Westphal, and P. Mahonen, "Performance Evaluation of IEEE 802.11-based WLANs in Vehicular Scenarios," in *IEEE Vehicular Technology Conference*, April 2007, pp. 1167–1171.

[23] S. Jaktheerangkoon, K. N. Nakorn, and K. Rojviboonchai, "Preliminary Performance Evaluation of IEEE 802.11-p in Blind Corner Scenario," *Int. Conference on Electrical Engineering/Electronics, Computer, Telecommunications and Information Technology*, 2016.

[24] L. Reichardt, T. Fugen, and T. Zwick, "Influence of Antennas Placement on Car-to-car Communications Channel," *European Conference on Antennas and Propagation*, pp. 630–634, 2009.

[25] S. Imai, K. Taguchi, T. Kashiwa, and T. Kawamura, "Effects of Car Body on Radiation Pattern of Car Antenna Mounted on Side Mirror for Inter-vehicle Communications," in *IEEE Antennas and Propagation Society International Symposium*, July 2014, pp. 601–602.

[26] S. Kaul, K. Ramachandran, P. Shankar, S. Oh, M. Gruteser, I. Seskar, and T. Nadeem, "Effect of Antenna Placement and Diversity on Vehicular Network Communications," in *IEEE Conference on Sensor, Mesh and Ad-Hoc Communications and Networks*, June 2007, pp. 112–121.

[27] P. Kukolev, A. Chandra, T. Mikulášek, and A. Prokeš, "Out of Vehicle Channel Sounding in 5.8 GHz Band," *Int. Workshop on Reliable Networks Design and Modeling*, no. October, pp. 341–344, 2015.

[28] L. Pinto, P. Santos, L. Almeida, and A. Aguiar, "Characterization and Modeling of the Bicycle-Antenna System for the 2.4 GHz ISM Band," in *IEEE Vehicular Networking Conference (VNC)*, Dec. 2018.

[29] F. Bai, D. D. Stancil, and H. Krishnan, "Toward Understanding Characteristics of Dedicated Short Range Communications (DSRC) from a Perspective of Vehicular Network Engineers," in *Int. Conference on Mobile Computing and Networking (MobiCom)*. New York, NY, USA: ACM, 2010, pp. 329–340.

[30] M. Boban, T. T. V. Vinhoza, M. Ferreira, J. Barros, and O. K. Tonguz, "Impact of Vehicles as Obstacles in Vehicular Ad Hoc Networks," *IEEE Journal on Selected Areas in Communications*, vol. 29, no. 1, pp. 15–28, January 2011.

[31] A. Morris, G. Hancox, O. Martin, D. Bell, C. Johansson, P. Rosander, J. Scholliers, and A. Silla, "Critical Accident Scenarios for Cyclists and How They Can Be Addressed Through ITS Solutions," in *International Cycling Safety Conference*, 2013.

[32] J. Kowalewski, T. Mahler, L. Reichardt, and T. Zwick, "Investigation of the Influence of Panoramic Roof on Mobile Telephony Antennas," in *European Conference on Antennas and Propagation (EuCAP)*, April 2014, pp. 1062–1066.

[33] A. Kwoczek, Z. Raida, J. Láčík, M. Pokorny, J. Puskelý, and P. Vágner, "Influence of Car Panorama Glass Roofs on Car2Car Communication," in *IEEE Vehicular Networking Conference*, Nov 2011, pp. 246–251.

[34] F. Neves, A. Cardote, R. Moreira, and S. Sargento, "Real-world Evaluation of IEEE 802.11P for Vehicular Networks," in *ACM Int. Workshop on Vehicular Inter-networking*, 2011, pp. 89–90.

[35] M. Boban, W. Viriyasitavat, and O. K. Tonguz, "Modeling Vehicle-to-vehicle Line of Sight Channels and Its Impact on Application-layer Performance," in *ACM Int. Workshop on Vehicular Inter-networking, Systems, and Applications (VANET)*, Taipei, Taiwan, 2013, pp. 91–94.

[36] B. C. Langford, J. Chen, and C. R. Cherry, "Risky Riding: Naturalistic Methods Comparing Safety Behavior from Conventional Bicycle Riders and Electric Bike Riders," *Accident Analysis & Prevention.*, vol. 82, pp. 220–226, 2015.